Water-Soluble Copolymers. 62. Nonradiative Energy Transfer Studies of pH- and Salt-Responsive Associations in Hydrophobically Modified, Hydrolyzed Maleic Anhydride–Ethyl Vinyl Ether Copolymers

Yuxin Hu, Michael C. Kramer, Chase J. Boudreaux, and Charles L. McCormick*

Department of Polymer Science, University of Southern Mississippi, Southern Station Box 10076, Hattiesburg, Mississippi 39406-0076

Received February 15, 1995; Revised Manuscript Received July 25, 1995[⊗]

ABSTRACT: A series of labeled, hydrophobically modified polymers based on the alternating copolymer of maleic anhydride and ethyl vinyl ether (MAEVE) has been synthesized to specifically address the issue of differences in domain organization of closed, polysoap systems and open, associative-thickening systems. Modification was achieved by reaction of primary amines with MAEVE in organic solvent and hydrolysis in aqueous base. This unique method allows stoichiometic modification with hydrophobic and fluorescent groups. Intramolecular associations predominate in a wide range of environments. The extent to which these interactions occur is effectively probed by monitoring nonradiative energy transfer (NRET) between naphthalene and pyrene groups covalently bound to the polymer chain. Intrapolymer NRET quantum efficiency increases with decreasing pH as the chain contracts to a globular conformation. Interpolymer NRET is independent of salt concentration, but intrapolymer NRET steadily increases with [NaCl] as the shielding of charge–charge repulsions constricts the coil. In extremely acidic and basic environments, interpolymer NRET increases as electrostatic repulsions are shielded or eliminated. A mechanism has been proposed whereby the compaction of labeled polymer micelles results in an enhancement in interpolymer aggregation due to the formation of hydrophobic micellar surfaces.

Introduction

In the past decade there have been a number of investigations in photophysics and photochemistry focusing on water-soluble polymers with pendent hydrophobic aromatic groups.[1–5] Amphiphilic polyelectrolytes functionalized by hydrophobic groups are of great interest because of their scientific and technological significance.[6] It is possible to elucidate the relationship between macroscopic and microscopic properties with photophysical techniques due to the sensitivity of "reporter" chromophores attached to the polymer chain. Changes in polymer conformation, microenvironment, and chain dynamics are reflected by the photophysical response.[7]

Maleic anhydride and some vinyl monomers are known to copolymerize to yield highly alternating structures.[8] These copolymers exhibit pH-responsive behavior in aqueous media. Hydrophobic vinyl mer units may aggregate to form organized domains with hydrophobic cores and charged interfaces. The hydrophilic maleic acid groups promote water solubility.[9,10] Morishima and Webber studied the photophysical behavior of poly(maleic acid-*alt*-vinylnaphthalene)[11–14] and poly(maleic acid-*alt*-vinylcarbazole)[15,16] and observed pH-dependent fluorescence behavior. Naphthalene excimer emission was shown to vary with pH as was the intensity of carbazole fluorescence emission. Energy transfer from carbazole[15,16] and naphthalene[11–14] to anthracene has also been studied.

Thomas and Strauss demonstrated that maleic acid/vinyl copolymers form a compact structure at low pH in aqueous solution via intramolecular hydrophobic association.[17–19] Such copolymers that aggregate intramolecularly to form micellar structures have been termed "polysoaps". Fluorescence quenching studies can be designed to effectively establish the domain size as a function of pH.[18,20] Strauss and co-workers have shown that the pK_a of poly(maleic acid-*alt*-butyl vinyl ether) is at a maximum at the transition from globular to open.[18,19,21]

Nonradiative energy transfer (NRET) is a useful technique for probing intramolecular associations and structural changes in polysoaps. The photophysical phenomenon of NRET between a donor and an acceptor covalently attached to a polymer has been termed "photon harvesting" by Webber *et al.*[3] and the "antenna effect" by Guillet *et al.*[22–24] NRET studies, for example, have been used to probe intramolecular association in polysoaps[9–20] as well as conformational changes and associations between polymer chains in intermolecularly associating systems.[24–31]

In this study, we consider the issues associated with structural effects on hydrophobic domain organization into intramolecular (closed) and intermolecular (open) aggregates. Elucidation of the mechanism of domain formation in these systems may allow precise tailoring of copolymers and terpolymers for use as polymeric surfactants and associative thickeners. Poly(maleic anhydride-*alt*-ethyl vinyl ether) (MAEVE) copolymers were covalently labeled with naphthalene (NRET donor) and pyrene (NRET acceptor) chromophores. Previous efforts have focused on variation of the vinyl ether to control polymer hydrophobicity,[19,21,32,33] but our research group has developed a homogeneous solution technique to stoichiometrically vary the incorporation of a hydrophobic moiety in the structure (Scheme 1).[34,35] With this technique, copolymers can readily be tailored from the same parent polymer to obtain a series of polymers with identical degrees of polymerization and varying hydrophobicity.

Viscosity, light scattering, and pyrene probe studies by our group have shown that there is a direct correlation between hydrophobicity and coil compaction. The intrinsic viscosity of hydrophobically modified, hydrolyzed MAEVE copolymers in aqueous solution has been

[⊗] Abstract published in *Advance ACS Abstracts,* September 1, 1995.

0024-9297/95/2228-7100$09.00/0

Scheme 1. Synthesis of Hydrophobically Modified Poly(sodium maleate-*alt*-ethyl vinyl ether)s

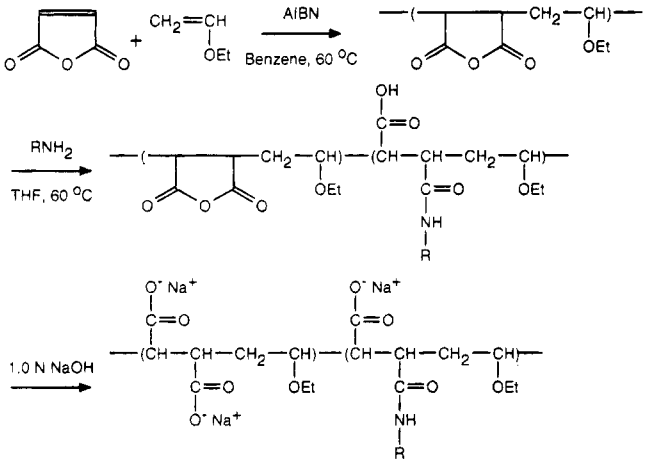

R = Octyl (C8), N1, N8, P2, P8

observed to drop precipitously as substitution with octyl or dodecyl groups is increased from 20 to 30 mol %.[35] This transition parallels the polyelectrolyte–polysoap transition in quaternized poly(4-vinylpyridine)s reported by Strauss.[36] As hydrophobicity increases, intramolecular hydrophobic associative forces predominate over electrostatic forces; as a result, the polymer coil contracts, and a hydrophobic, micellar microdomain forms.

MAEVE copolymer was modified with 30 mol % octylamine prior to hydrolysis in aqueous base. At this modification level, MAEVE forms a compact structure in water, as determined by rheological studies. Excimer emission studies of naphthalene-labeled MAEVE indicated that octyl incorporations up to 30 mol % allow sufficient microdomain fluidity for formation of the dimeric excited state.[35] Thus, the responsiveness of micellar domains to various environmental stimuli should be optimal. The copolymer was fluorescently labeled with 2-(1-pyrenylsulfonamido)ethylamine and 8-(1-pyrenylsulfonamido)octylamine as energy transfer acceptors; the energy transfer donors 1-naphthylmethylamine and 7-(1-naphthylmethoxy)heptylamine were also incorporated.

The naphthalene/pyrene energy transfer pair has been successfully employed by Winnik[28,29] to investigate NRET enhanced by the thermoreversible phase transition of aqueous solutions of pyrene- and naphthalene-labeled poly(*N*-isopropylacrylamide). Webber[37] utilized NRET studies to detect steric hindrance effects in pyrene-labeled poly(2-vinylnaphthalene). In this study, naphthalene and pyrene chromophores are covalently attached to poly(sodium maleate-*alt*-ethyl vinyl ether). The characterization of polymers labeled with these chromophores is described herein. NRET is measured in mixed solutions of polymer singly labeled with naphthalene or pyrene to evaluate intermolecular associations, and intramolecular associations are probed by NRET studies of doubly labeled polymers. The photophysical response is determined in aqueous solution as a function of pH and electrolyte (NaCl) concentration. Results are compared with respect to changes in these parameters and in chromophore spacer length.

Experimental Section

Materials. All commercial chemicals and solvents were purchased from Aldrich Chemical Co. (Milwaukee, WI). Benzene and tetrahydrofuran (THF) were dried over calcium hydride and distilled under nitrogen. Maleic anhydride was recrystallized twice from chloroform; ethyl vinyl ether (bp 32–33.5 °C) was distilled twice at atmospheric pressure before use.

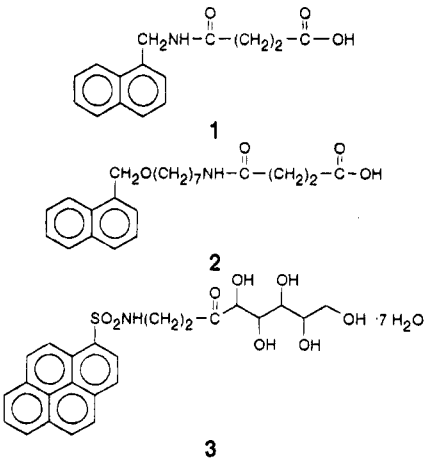

Figure 1. Model compounds **1**–**3**.

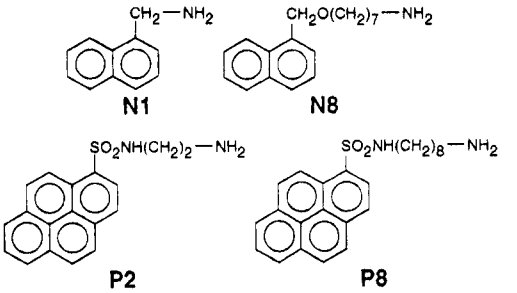

Figure 2. Fluorescent polymer labels N1, N8, P2, and P8.

2,2′-Azobis(2-methylpropionitrile) (AIBN) was recrystallized from methanol. Other materials were used as received. Water was deionized and possessed a conductance < 10^{-7} Ω^{-1}/cm.

Succinic Acid *N*-(1-Naphthylmethyl) Monoamide (1). The structures of model compounds **1**–**3** are shown in Figure 1. Into a 25 mL round-bottomed flask fitted with a magnetic stirring bar, N_2 inlet, and bubbler was added succinic anhydride (1.0 g, 10 mmol) dissolved in 10 mL of DMF. A solution of 1-naphthylmethylamine (1.3 g, 8.3 mmol) in 3 mL of DMF was then added. The reaction mixture was allowed to stir for 1 h at room temperature. The slurry was then precipitated in water, and pale brown solids were recovered by vacuum filtration. The solid product was then crystallized from boiling water after treatment with activated charcoal: mp 172–174 °C; ^{13}C NMR (DMSO-d_6) δ 29.2, 30.0, 40.2, 123.4, 125.3, 125.7, 126.1, 127.4, 128.4, 130.8, 133.2, 134.6, 171.0, 173.9.

Succinic Acid *N*-[7-(1-Naphthylmethoxy)heptyl] Monoamide (2). Model compound **2** was synthesized using the methods of McCormick and Chang.[35]

***N*-[2-(1-Pyrenylsulfonamido)ethyl]gluconamide Heptahydrate (3).** Model compound **3** was synthesized and characterized according to the literature.[38]

7-(1-Naphthylmethoxy)heptylamine (N8). The structures of the chromophores utilized for fluorescent labeling are shown in Figure 2. Labeling is accomplished by acylation of these primary amines with the maleic anhydride repeat units of poly(maleic anhydride-*alt*-ethyl vinyl ether). Label N1 (1-naphthylmethylamine) is commercially available and was used as received. The synthesis of N8 label outlined by McCormick and Chang[35] was followed.

2-(1-Pyrenylsulfonamido)ethylamine (P2) and 8-(1-Pyrenylsulfonamido)octylamine (P8). Methods employed by Ezzell and McCormick[38] were utilized for the syntheses of both pyrene labels.

Poly(maleic anhydride–ethyl vinyl ether) [Poly(MA-*alt*-EVE)].[35] The synthesis of the parent polymer and subsequent modifications are depicted in Scheme 1. Maleic anhydride (65.0 g, 663 mmol) was dissolved in 600 mL of benzene at 60 °C in a 1 L round-bottomed flask equipped with a condenser, septa, magnetic stirring bar, and N_2 purge. After 0.20 g of AIBN (1.2 mmol) was added, ethyl vinyl ether (49.0 g, 680 mmol) was immediately injected into the solution. The solution was stirred at 60 °C overnight, and the white

precipitate that formed was isolated by vacuum filtration. The copolymer was purified by repeated dissolution in acetone and precipitation in diethyl ether. The M_w of poly(MA-*alt*-EVE) was 2.2×10^5 g/mol, which was measured with a light scattering spectrophotometer.

Naphthalene- and Pyrene-Labeled Poly(sodium maleate-*alt*-ethyl vinyl ether)s. Solutions of octylamine (1.1 g, 8.5 mmol) and chromophore in 20 mL of THF were added dropwise into a rapidly stirring solution of poly(MA-*alt*-EVE) (5.0 g, 30 mmol) in 150 mL of THF at room temperature under nitrogen. After 24 h of reflux at 66 °C, the polymers were precipitated in 1 L of diethyl ether. The polymers were purified by repeated dissolution in THF and precipitation in diethyl ether.

Hydrolyses of unreacted anhydride groups were carried out in 100 mL of aqueous 1.0 N NaOH. After the polymers completely dissolved, the solutions were dialyzed against deionized water at room temperature with Spectra-Por dialysis tubing (12 000–14 000 g/mol molecular weight cutoff). When a constant, neutral pH was attained, the solutions were freeze-dried. The structures of the polymers synthesized are shown in Scheme 1. Copolymer compositions are shown in Table 1.

Instrumentation. A Bruker AC-200 NMR spectrometer was used to determine ^1H, ^{13}C, and gated-decoupled ^{13}C NMR spectra. NMR spectra were determined either in acetone-d_6 with 1% (v/v) TMS as an internal standard for unhydrolyzed polymer or in deuterium oxide with 1% (w/w) DSS as an internal standard for hydrolyzed polymers. The M_w of poly(MA-*alt*-EVE) was obtained with a Brookhaven BI-DS low-angle laser light scattering spectrophotometer. UV–vis spectra were recorded with a Hewlett-Packard 8452A diode array spectrophotometer. Steady-state fluorescence spectra were measured on a Spex Fluorolog-2 fluorescence spectrometer equipped with a DM3000F data system.

Solution Preparation and Fluorescence Measurements. Polymer stock solutions were prepared with a concentration of 1.00 g/L at room temperature. These were allowed to stand for 24 h before dilution to a known concentration. All polymer solutions were diluted to 0.05 g/L (50 ppm) prior to fluorescence measurements. For the pH studies, 0.1 N HCl and 0.1 N NaOH aqueous solutions were used to adjust the solution pH. For the salt studies, 0.5 M aqueous NaCl was added to polymer solutions.

For UV–vis absorption measurements, water was used as a blank. All solutions were degassed by vigorous bubbling with nitrogen for 15 min before fluorescence measurement. All emission and excitation spectra were corrected. Slit widths were set at 2.0 and 1.0 mm at the fluorescence excitation and emission positions, respectively. For NRET measurements, 290 nm was chosen as the excitation wavelength. Pyrene chromophores were singly excited at 335 nm to observe pyrene fluorescence emission. Quantum yields (Φ) were calculated by integration of peak areas of corrected spectra (in wavenumber units) referenced to 2-aminopyridine in 0.10 N H_2SO_4 as a standard ($\Phi = 0.60$ at 290 nm excitation wavelength).[39] Beer's law corrections were applied for optical density changes at the excitation wavelength. Corrections were also made for refractive index differences. Quantum efficiencies of naphthyl/pyrene energy transfer were determined by integration of corrected emission spectra from 310 to 370 nm (naphthyl emission) and from 370 to 550 nm (pyrene emission). For pyrene emission spectra excited at 290 nm in the presence of the naphthalene label, naphthyl emission was taken into account by subtraction of C8-N1 and C8–N8 spectra at identical naphthalene concentrations and environments ([NaCl], pH).

Results and Discussion

Polymer Characterization. Poly(maleic anhydride-*alt*-ethyl vinyl ether) was synthesized by a previously utilized procedure.[35] A copolymer with a completely alternating structure was obtained as confirmed by gated-decoupled ^{13}C NMR. The modifier feed consisted of 30 mol % octylamine and 1 mol % chromophore with respect to anhydride groups. From Table 1, it is readily apparent that near-quantitative chromophore incorporation onto the poly(MA-*alt*-EVE) backbone is obtained. Polymers are named according to their hydrophobe content. All copolymers contain 30 mol % octyl groups. The suffixes N and P denote naphthalene and pyrene substitution, respectively. The numbers following N and P indicate the modifying chromophore used; this number describes the number of carbons contained in the aliphatic spacer. Naphthalene and pyrene incorporation were determined by UV–vis absorbance studies of aqueous polymer solutions. Label molar absorptivities are assumed to equal that of their model compounds (Table 2).

Table 1. Copolymer Compositions

polymer	C8 content (mol %)[a]	naphthalene content (mol %)[b]	pyrene content (mol %)[b]
C8	30		
C8-N1	31	1.0	
C8-P2	30		0.99
C8-N1-P2	30	1.2	0.99
C8-N8	32	1.1	
C8-P8	29		0.96
C8-N8-P8	30	1.1	0.96

[a] From gated-decoupled ^{13}C NMR (D_2O) data. [b] From UV absorption data.

Table 2. Model Compound Molar Absorptivities

model compound	fluorophore	ϵ (M^{-1} cm^{-1})
1	naphthalene	6780[a]
2	naphthalene	6730[a]
3	pyrene	24100[b]

[a] Molar absorptivity at λ_{max} (282 nm). [b] Molar absorptivity at λ_{max} (350 nm).

Table 3. Solutions Prepared for Energy Transfer Experiments[a]

Short-Spacer Chromophores

solution	[C8] (ppm)	[C8-N1] (ppm)	[C8-P2] (ppm)	[C8-N1-P2] (ppm)	[naphthalene] (μmol/L)	[pyrene] (μmol/L)
C8-N1	25	25			0.99	
C8-P2	25		25			0.95
C8-N1/ C8-P2		25	25		0.99	0.95
C8-N1-P2	25			25	1.1	0.94

Long-Spacer Chromophores

solution	[C8] (ppm)	[C8-N8] (ppm)	[C8-P8] (ppm)	[C8-N8-P8] (ppm)	[naphthalene] (μmol/L)	[pyrene] (μmol/L)
C8-N8	25	25			1.0	
C8-P8	25		25			0.92
C8-N8/ C8-P8		25	25		1.0	0.92
C8-N8-P8	25			25	1.0	0.91

[a] All total polymer concentrations equal 50 ppm.

Although the copolymerization of maleic anhydride with ethyl vinyl ether is a virtually alternating process,[8] substitution of hydrophobe and fluorescent label onto the polymer chain is random due to the similar reactivities of the primary amine groups on the modifiers. The random microstructure is also attributable to the homogeneity of the substitution medium. From the molecular weight of the parent copolymer, an average incorporation of 900 unsubstituted, 13 pyrene, 14 naphthalene, and 390 octyl groups per chain is inferred.

Spectroscopic Characterization. Solutions of naphthalene- and pyrene-labeled polymer were mixed with solutions of polymer C8 (unlabeled polymer) to adjust polymer concentrations (Table 3). Solutions were named according to the fluorescently labeled polymers employed. For example, C8-N1/C8-P2 is a mixed solution of singly labeled naphthalene polymer and singly labeled pyrene polymer. C8-N1-P2 is a solution of polymer doubly labeled with both naphthalene and

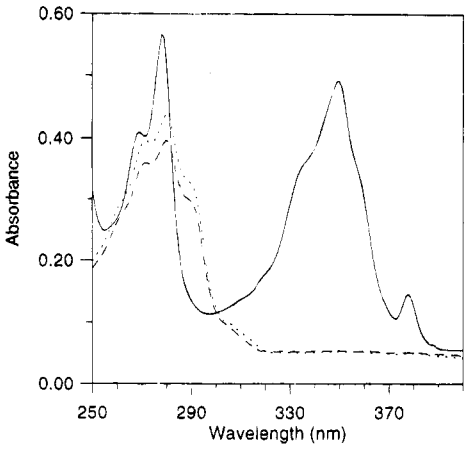

Figure 3. UV–vis absorption spectra of naphthyl model compounds **1** (···) and **2** (– – –) and pyrenyl model compound **3** (—). [**1**], [**2**] = 50 μM. [**3**] = 20 μM.

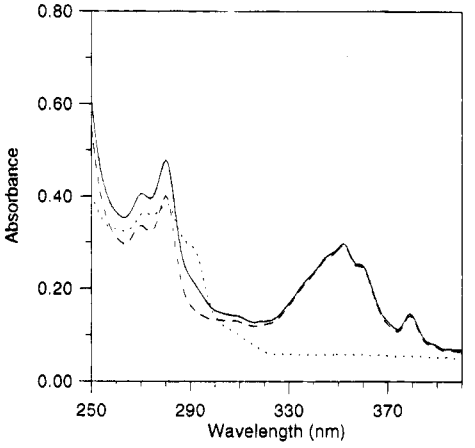

Figure 4. UV–vis absorption spectra of labeled polymers C8-N8 (···), C8-P8 (– – –), and C8-N8-P8 (—). Sample concentration: 1000 ppm. pH: 7.

pyrene. Polymer C8 was added to adjust all polymer concentrations to 50 ppm. The total absorbances of the polymer solutions at the excitation wavelengths (290 and 335 nm) were kept below 0.05 to avoid energy transfer by radiative processes.

The UV–vis absorption spectra of model compounds **1**–**3** are shown in Figure 3, and spectra of C8-N8, C8-P8, and C8-N8-P8 are shown in Figure 4. A pyrene absorbance minimum is centered around 290 nm, as is an absorbance shoulder of the naphthalene chromophore. In order to maximize NRET between naphthyl and pyrene chromophores, an excitation wavelength of 290 nm is employed. This allows preferential excitation of naphthalene chromophores in the presence of pyrene. At 290 nm, the fraction P of the total light absorbed by naphthyl chromophores in the presence of pyrene was calculated using eq 1, in which $A_N(\lambda)$ and $A_{Py}(\lambda)$ are the absorbances of naphthalene and pyrene at wavelength λ (290 nm).[40]

$$P = \frac{1 - 10^{-A_N(\lambda)}}{2 - 10^{-A_N(\lambda)} - 10^{-A_{Py}(\lambda)}} \quad (1)$$

At 290 nm, naphthyl chromophores are responsible for 50% of the total light absobed by solutions of C8-N1 and C8-P2 at N1/P2 = 1.1; the naphthyl chromophores are responsible for 52% of the total light absorbed by polymer solutions labeled with long-spacer chromophores at N8/P8 = 1.1.

Figure 5 shows the overlap between the UV–vis absorption spectrum of pyrene model compound **3** and the corrected fluorescence of naphthalene model com-

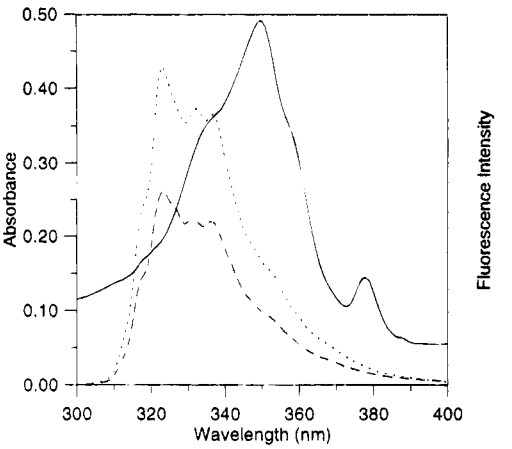

Figure 5. Spectral overlap of pyrenyl model compound **3** UV–vis absorbance (—) with fluorescence emission of naphthyl model compounds **1** (···) and **2** (– – –). Excitation wavelength: 290 nm. pH: 7. [**1**], [**2**] = 50 μM. [**3**] = 20 μM.

pounds **1** and **2**. The spectral data demonstrate good overlap between naphthalene label emission and pyrene label absorption. This overlap is requisite for nonradiative energy transfer from donor (naphthalene) to acceptor (pyrene). According to Förster,[41] the characteristic distance R_0 between donor and acceptor at which half of the excitation energy is transferred is given by the equation

$$R_0 = \left(\frac{9000(\ln 10)\,\kappa^2\,\Phi_D^0}{128\,\pi^5 n^4 N}\int_0^\infty \lambda^4\, I(\lambda)\,\epsilon(\lambda)\,d\lambda\right)^{1/6} \quad (2)$$

where κ^2 is a function of the mutual orientation of donor and acceptor with $\kappa^2 = {}^2/_3$ for random orientation in fluid media, Φ_D^0 is the emission quantum yield of the donor in the absence of acceptors, n is the solvent refractive index, and N is Avogadro's number. The integral depicted in eq 2 is the overlap integral, where $I(\lambda)$ is the normalized fluorescence emission intensity such that

$$\int_0^\infty I(\lambda)\,d\lambda = 1 \quad (3)$$

and $\epsilon(\lambda)$ is the molar absorptivity of the acceptor as a function of the wavelength λ. The sixth-power dependence results from dipole–dipole interactions that govern nonradiative energy transfer. The quantum yields of the model compounds are $\Phi_D^0 = 0.10$ for naphthalene model **1**, $\Phi_D^0 = 0.066$ for naphthalene model **2**, and $\Phi_A^0 = 0.73$ for pyrene model **3**. These were obtained by comparison of the integrated emission intensities of aqueous solutions of model compounds excited at 290 nm with that of 2-aminopyridine in 0.10 N H_2SO_4 ($\Phi = 0.60$ at 290 nm excitation wavelength).[39] The overlap integral between naphthalene model **1** and pyrene model **3** was determined to be 19.05×10^{-15} cm^6 mol^{-1}; the naphthalene model **2**/pyrene model **3** overlap integral is 17.08×10^{-15} cm^6 mol^{-1}. In aqueous media, these data correspond to $R_0 = 26.6$ Å for naphthalene model **1**/pyrene model **3** and $R_0 = 24.7$ Å for naphthalene model **2**/pyrene model **3**.

There are several useful methods for characterization of NRET between fluorescence donor and acceptor. Morawetz used the fluorescence intensity ratio of donor to acceptor to describe NRET in polymer systems.[4] Guillet[22–24] defined the quantum efficiency of NRET, χ, as

$$\frac{\chi}{1-\chi} = \frac{\Phi_D^0 I_A}{\Phi_A^0 I_D} \quad (4)$$

where Φ_D^0 is the fluorescence emission quantum yield

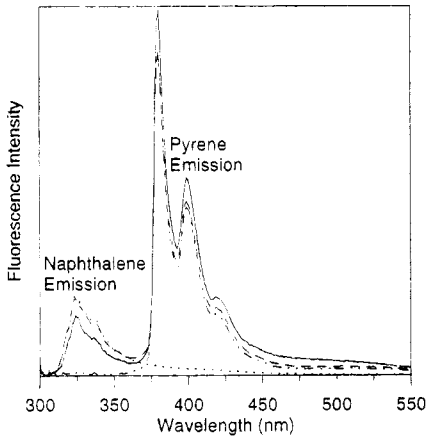

Figure 6. Fluorescence spectra of long-spacer labeled polymers C8-N8 (···), C8-P8 (– ··), C8-N8-P8 (– – –), and C8-N8/C8-P8 (—). Excitation wavelength: 290 nm. Polymer concentration: 50 ppm. pH: 7.

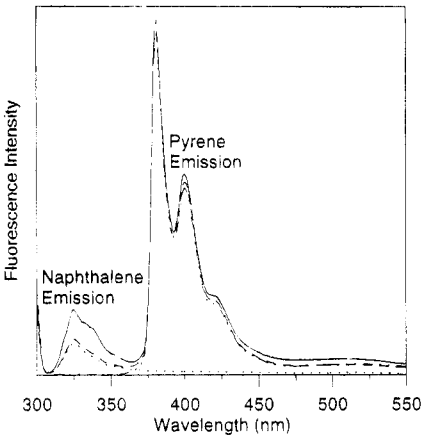

Figure 7. Fluorescence spectra of short-spacer labeled polymers C8-N1 (···), C8-P2 (– ··), C8-N1-P2 (– – –), and C8-N1/C8-P2 (—). Excitation wavelength: 290 nm. Polymer concentration: 50 ppm. pH: 7.

of donor on the polymer singly labeled with donor and Φ_A^0 is the fluorescence quantum yield of the acceptor on the polymer doubly labeled with donor and acceptor upon direct excitation. I_D and I_A are the integrated emission intensities of donor and acceptor, respectively, on the doubly labeled polymer. Here the fluorescence emission quantum yields of naphthalene on singly labeled polymers were used to express Φ_D^0 and the fluorescence emission quantum yields of pyrene on singly labeled polymers were used to express Φ_A^0. Guillet[22-24] studied the naphthalene/anthracene donor/acceptor pair with an excitation wavelength of 280 nm where the extinction coefficient of anthracene is so low that its emission is negligible. However, in the studies discussed here, 290 nm is used as the excitation wavelength for the naphthyl/pyrene energy transfer pair, and both chromophores are excited at this wavelength. The expression of the quantum efficiency χ of energy transfer modified for this case is

$$\frac{\chi}{1-\chi} = \frac{\Phi_D^0(I_A - I_A^0)}{\Phi_A^0 I_D} \tag{5}$$

where I_A^0 is the integrated fluorescence emission of the polymer singly labeled with pyrene. The quantum yields of pyrene in the doubly labeled polymers should be similar. This is supported by the similarity in pyrene emission intensities when samples are excited at 335 nm.

Figure 6 shows the corrected fluorescence spectra of C8-N8, C8-P8, C8-N8-P8, and C8-N8/C8-P8 in aqueous solution at 50 ppm total polymer concentration. Naphthalene excimer emission was not observed, but a small structureless emission centered at about 520 nm is observed in polymers labeled with pyrene. This band is observed when excitation wavelengths of both 290 and 335 nm are employed and arises from pyrene excimer emission. The emission intensity of naphthyl chromophores in C8-N8/C8-P8 from 310 to 370 nm is lower than that of singly labeled polymer (C8-N8) and of doubly labeled polymer (C8-N8-P8). Interpolymer quenching of naphthalene via nonradiative energy transfer from excited state naphthalene to ground state pyrene is responsible for this behavior.

Fluorescent labels possessing short alkyl spacers do not exhibit interpolymer NRET to the extent that the long-spacer systems do since the molecular motions of N1 and P2 chromophores are not decoupled from the polymer backbone to the same extent as N8 and P8.

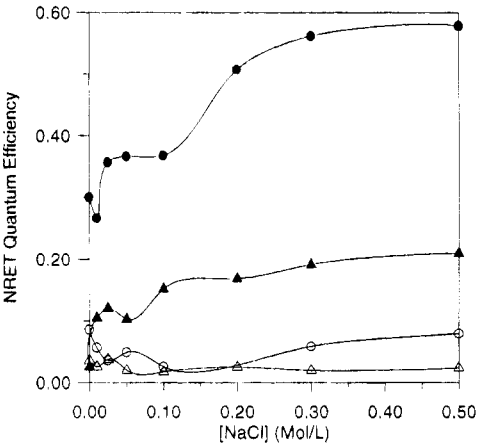

Figure 8. NRET quantum efficiency of C8-N1/C8-P2 (△), C8-N8/C8-P8 (○), C8-N1-P2 (▲), and C8-N8-P8 (●) as a functiion of sodium chloride concentration. Polymer concentration: 50 ppm. pH: 7.

Naphthalene concentration is slightly higher in solutions of C8-N1-P2 (1.1 μM) than in other solutions of the short-spacer naphthalene-labeled series. However, the intensity of naphthalene emission in solution C8-N1-P2 at 310–370 nm is less than that of C8-N1/C8-P2 (Figure 7). Labels associate intramolecularly at the expense of intermolecular interactions, and intramolecular NRET is more pronounced as evidenced by reduced quenching of naphthalene emission in C8-N1/C8-P2 mixed polymer solution.

Salt Effects on NRET. The effect of sodium chloride on NRET quantum efficiency as a function of spacer length and association type is shown in Figure 8. NRET is most prevalent in the doubly labeled polymer series C8-N1-P2 and C8-N8-P8 (closed symbols) throughout the entire NaCl concentration range. NRET steadily increases with ionic strength. Viscosity studies indicate a reduction in coil dimensions. As this occurs, the average chromophore separation decreases and the contraction is observed as an increase in NRET.

A gradual NRET increase with NaCl concentration is observed for both C8-N1-P2 and C8-N8-P8 (Figure 8, closed symbols). Mixed solutions of singly labeled polymers show low, virtually unchanging NRET values. When NRET donor and acceptor chromophores are present on the same polymer chain, the photophysical response is more prominent. As polymer coil dimensions shrink with increasing ionic strength, the average intramolecular label separation decreases. This phenomenon is illustrated schematically in Figure 9.

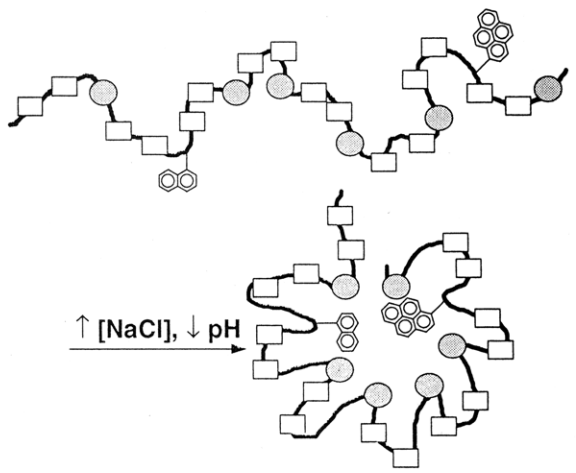

Figure 9. Coil contraction-triggered intramolecular NRET increase.

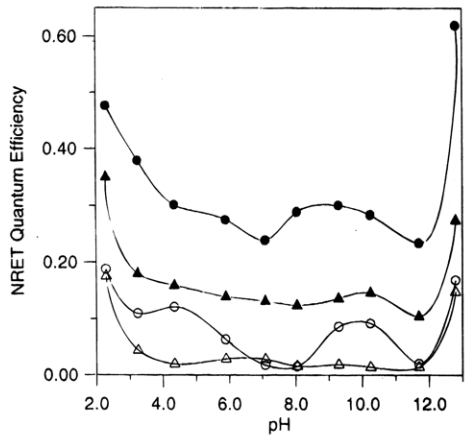

Figure 10. NRET quantum efficiency of C8-N1/C8-P2 (△), C8-N8/C8-P8 (○), C8-N1-P2 (▲), and C8-N8-P8 (●) as a function of pH. Polymer concentration: 50 ppm.

pH Effects on NRET. The quantum efficiency of intra- and interpolymer energy transfer between naphthalene and pyrene as a function of pH is shown in Figure 10. Energy transfer data from mixed solutions of singly labeled polymers (C8-N1/C8-P2 and C8-N8/C8-P8) are depicted by open symbols, and data from solutions of doubly labeled polymers (C8-N1-P2 and C8-N8-P8) are represented by closed symbols. For this polymer series, the molar ratio of carboxylic acid groups to hydrophobic groups is about 5.5 to 1. The acid functionality helps to impart water solubility and pH sensitivity.

A significant feature of Figure 10 is the high values of intrapolymer NRET relative to interpolymer NRET throughout the entire pH range. This is seen as an enhancement in C8-N1-P2 and C8-N8-P8 NRET quantum efficiency (closed symbols) relative to NRET in mixed singly labeled solutions (C8-N1/C8-P2 and C8-N8/C8-P8, open symbols). This suggests that intramolecular hydrophobic associations prevail over a wide pH range. The charge density along the polymer chain is a function of pH. As pH decreases, the reduction in electrostatic repulsions shrinks the polymer coil. For all polymers and solutions, the quantum efficiency of energy transfer increases below pH 5. As pH is increased, the electrostatic repulsions result in reduced intramolecular associations. The most dramatic changes in NRET quantum efficiency are observed in doubly labeled polymers C8-N1-P2 and C8-N8-P8 (Figure 10, closed symbols). NRET decreases ≥ 50% as pH is increased from 2 to 6 for both C8-N1-P2 and C8-N8-P8. As the coil is opened by Coulombic repulsions, the distance between chromophores increases, and intramolecular NRET decreases. This trend is in agreement with previous studies.[34,35]

A maximum in NRET quantum efficiency occurs in mixed solutions of singly labeled long-spacer polymer C8-N8/C8-P8 at pH 9–10 (Figure 10). This indicates an enhancement in interpolymer associations in this pH range. As the chain expands, intrapolymer associations are broken up and interpolymer interactions increase. The long alkyl spacer group decouples the motion of the naphthalene and pyrene groups from that of the polymer backbone, providing an effective mode of hydrophobe diffusion to form interpolymer aggregates. This result is supported by previous viscosity studies that indicate maxima in reduced viscosity around pH 9.5 for octylamido-modified poly(sodium maleate-*alt*-ethyl vinyl ether)s.[35] Because most or all of the carboxylic acid groups are neutralized at high pH, further base addition increases the ionic strength. The shielding of Coulombic repulsions collapses the polymer coil, and an increase in intrapolymer associations is observed as an NRET enhancement in solutions of doubly labeled polymers C8-N1-P2 and C8-N8-P8 at pH > 10 (closed symbols).

At extremes in pH, intermolecular NRET increases, thus signifying the onset of an aggregative process. As pH decreases from 6 to 2, naphthalene/pyrene NRET between polymer chains in the C8-N1/C8-P2 and C8-N8/C8-P8 systems increases (open symbols). Migration of hydrophobic groups to the polymer micelle surface may account for this behavior. Strauss reported intermolecular association and gel formation in aqueous solutions of highly quaternized (38 mol % dodecyl modification) poly(vinylpyridine).[36] It was postulated that added electrolyte helps to shield Coulombic forces between pyridinium groups and that a fraction of the surface of a polymer micelle then becomes occupied by hydrophobic groups. Polymer–polymer aggregation would then become more favorable. The elimination of electrostatic repulsions may also lead to the formation of a hydrophobic surface.

Intermolecular aggregation in polysoaps has been verified by viscosity studies.[36] Viscosity increases markedly with ionic strength, and there is a time dependence on viscosity as well. Over long periods of time, the viscosity of a freshly diluted sample decreases to an equilibrium value. This result implies a gradual breakup of polymer aggregates over time. Chang and McCormick reported similar phenomena in MAEVE copolymers modified with dodecyl groups.[35] Viscosity was found to diminish over a period of 1 week, and the decrease was most pronounced in the more highly substituted polymers; intramolecular organization of micellar domains with the breakup of intermolecular associations drives this response. Time-dependent aging was not observed in the rheological behavior of octyl-modified MAEVE, but marked increases in intermolecular associations are seen by NRET analysis at low and high pH. Although viscometric data do not report aggregation, the photophysical response reveals that multimer aggregates do indeed form. This is shown schematically in Figure 11. At the onset of interpolymer association, hydrophobic interactions occur between donor and acceptor chromophores on different polymer chains. As a result, the average distance between donor and acceptor decreases, and NRET quantum efficiency increases.

Ionic strength effects may account for hydrophobic micelle surface formation and aggregation. At high pH, as the electrostatic repulsions on the polymer micelle

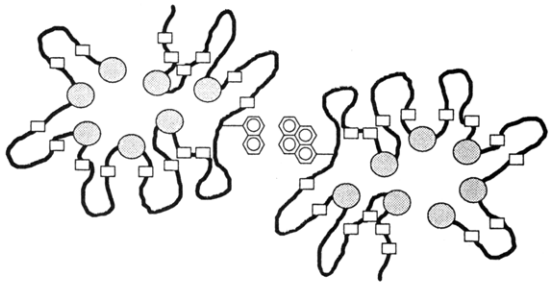

Figure 11. Proposed mechanism of acid-induced intermolecular NRET enhancement via exposure of hydrophobic groups to polymer micelle surface.

surface are shielded by added base, a fraction of the hydrophobic groups are exposed to the surface. As a result, NRET enhancement in mixed solutions of singly labeled polymers C8-N1/C8-P2 and C8-N8/C8-P8 is observed at pH > 11 (open symbols).

NRET Donor/Acceptor Ratio Effects. When the ratio of naphthalene to pyrene is changed, NRET quantum efficiency may change. Winnik has reported an NRET enhancement in mixed solutions of fluorescently labeled, hydrophobically modified poly(*N*-isopropylacrylamide) (PNIPAM). NRET was observable at very low polymer concentrations and is reflective of the formation of intermolecular aggregates that were verified by quasi-elastic light scattering studies.[42] As the naphthalene/pyrene ratio is increased from 1 to 5 in C8-N8/C8-P8 mixed solutions, NRET efficiency also increases. Even at very low polymer concentrations, the highly mobile, long-spacer labels can diffuse to a sufficient degree to form intermolecular aggregates. Label mobility appears to be a prerequisite for efficient NRET.

Conclusions

A series of fluorescently labeled poly(sodium maleate-*alt*-ethyl vinyl ether)s containing 30% octyl groups have been synthesized by a novel technique that allows stoichiometric control of polymer hydrophobicity. Polymers were singly labeled with 1 mol % of either naphthalene (donor) or pyrene (acceptor) chromophores for intermolecular nonradiative energy transfer (NRET) studies; polymers were also doubly labeled with 1 mol % of naphthalene and pyrene for intramolecular NRET analysis. Rheological studies have shown that intramolecular associations predominate at the low polymer concentrations employed, but steady-state fluorescence emission studies support naphthalene/pyrene energy transfer within and between hydrophobic domains. As electrolyte concentration increases, closed associations and intramolecular NRET are enhanced due to the shielding of electrostatic repulsions that expand the polymer coil. Intrapolymer hydrophobic association and NRET are also augmented at low pH due to the elimination of electrostatic repulsive forces.

A mechanism involving the formation of a hydrophobic micellar surface has been postulated to account for the intermolecular associative behavior observed by NRET measurement at low and high pH. Polymer–polymer aggregation that is not observable by viscosity studies is readily probed by NRET measurements of mixed solutions of polymer singly labeled with donor or acceptor. Chromophores separated from the polymer backbone by longer spacer lengths tend to interact to a greater extent, as reflected in the photophysical behavior of these systems. NRET enhancement with increasing [Na]/[Py] for the long-spacer labeled systems supports intermolecular domain association in addition to intramolecular association at low polymer concentrations.

Acknowledgment. Funding from Mobil Corp., the U.S. Department of Energy, and the U.S. Office of Naval Research is gratefully acknowledged.

References and Notes

(1) Morishima, Y. *Prog. Polym. Sci.* **1990**, *15*, 949.
(2) Turro, N. J.; Gratzel, M.; Braun, M. *Angew. Chem., Int. Ed. Engl.* **1980**, *19*, 675.
(3) Webber, S. E. *Chem. Rev.* **1990**, *90*, 1469.
(4) Morawetz, H. *Science* **1988**, *240*, 172.
(5) Nagata, I.; Morawetz, H. *Macromolecules* **1981**, *14*, 87.
(6) *Water-Soluble Polymers: Synthesis, Solution Properties, and Applications*; Shalaby, S. W., McCormick, C. L., Butler, G. B., Eds.; ACS Symposium Series No. 467; American Chemical Society: Washington, DC, 1991.
(7) *Photophysical and Photochemical Tools in Polymer Science*; Winnik, M. A., Ed.; D. Reidel: Dordrecht, Holland, 1986.
(8) *Polymers as Rheology Modifiers*; Schulz, D. N., Glass, J. E., Eds.; ACS Symposium Series No. 462; American Chemical Society: Washington, DC, 1991.
(9) Morishima, Y.; Itoh, Y.; Nozakura, S. *Makromol. Chem.* **1981**, *182*, 3135.
(10) Morishima, Y.; Itoh, Y.; Nozakura, S. *Macromolecules* **1984**, *17*, 2264.
(11) Morishima, Y.; Kobayashi, T.; Nozakura, S.; Webber, S. E. *Macromolecules* **1987**, *20*, 807.
(12) Bai, F.; Webber, S. E. *Macromolecules* **1988**, *21*, 628.
(13) Morishima, Y.; Lim, H. S.; Nozakura, S.; Sturtevant, J. L. *Macromolecules* **1989**, *22*, 1148.
(14) Sturtevant, J. L.; Webber, S. E. *Macromolecules* **1989**, *22*, 3564.
(15) Itoh, Y.; Nakada, M.; Satoh, H.; Hachimori, A.; Webber, S. E. *Macromolecules* **1993**, *26*, 1941.
(16) Itoh, Y.; Satoh, H.; Yasue, T.; Hachimori, A.; Satozano, H.; Suzuki, S.; Webber, S. E. *Macromolecules* **1994**, *27*, 1434.
(17) Chu, D. Y.; Thomas, J. K. *Macromolecules* **1987**, *20*, 2133.
(18) Zdanowicz, V. S.; Strauss, U. P. *Macromolecules* **1993**, *26*, 4770.
(19) Strauss, U. P.; Vesnaver, G. *J. Phys. Chem.* **1975**, *79*, 1558.
(20) Binana-Limbelé, W.; Zana, R. *Macromolecules* **1990**, *23*, 2731.
(21) Strauss, U. P.; Vesnaver, G. *J. Phys. Chem.* **1975**, *79*, 2462.
(22) Ng, D.; Guillet, J. E. *Macromolecules* **1982**, *15*, 724.
(23) Holden, D. A.; Guillet, J. E. *Macromolecules* **1980**, *13*, 289.
(24) Guillet, J. E.; Rendall, W. A. *Macromolecules* **1986**, *19*, 224.
(25) Major, M. D.; Torkelson, J. M.; Brearley, A. M. *Macromolecules* **1990**, *23*, 1700.
(26) Nagata, I.; Morawetz, H. *Macromolecules* **1981**, *14*, 87.
(27) Ito, S.; Ohmori, S.; Yamamoto, M. *Macromolecules* **1992**, *25*, 185.
(28) Winnik, F. M. *Macromolecules* **1989**, *22*, 734.
(29) Winnik, F. M. *Polymer* **1990**, *31*, 2152.
(30) Schild, H. G.; Tirrell, D. A. *Macromolecules* **1992**, *25*, 4553.
(31) Fox, R. B.; Price, T. R.; Cozzens, R. F.; Echols, W. H. *Macromolecules* **1974**, *7*, 937.
(32) Strauss, U. P.; Schlesinger, M. S. *J. Phys. Chem.* **1978**, *82*, 1627.
(33) Strauss, U. P.; Schlesinger, M. S. *J. Phys. Chem.* **1978**, *82*, 571.
(34) McCormick, C. L.; Hoyle, C. E.; Clark, M. D. *Polymer* **1992**, *33*, 243.
(35) McCormick, C. L.; Chang, Y. *Macromolecules* **1994**, *27*, 2151.
(36) Strauss, U. P.; Gershfeld, N. L.; Crook, E. H. *J. Phys. Chem.* **1956**, *60*, 577.
(37) Hargreaves, J. S.; Webber, S. E. *Macromolecules* **1982**, *15*, 424.
(38) Ezzell, S. A.; McCormick, C. L. *Macromolecules* **1992**, *25*, 1881.
(39) Rusakowicz, R.; Testa, A. C. *J. Phys. Chem.* **1968**, *72*, 2680.
(40) Lin, G.; Guillet, J. E. *Macromolecules* **1990**, *23*, 1388.
(41) Förster, T. *Discuss. Faraday Soc.* **1959**, *27*, 7.
(42) Ringsdorf, H.; Simon, J.; Winnik, F. M. *Macromolecules* **1992**, *25*, 5353.

MA950198L